Mumford-Shah Based Unsupervised Segmentation of Brain Tissue on MR Images

A. Cevik[1] and B.M. Eyuboglu[1,2]

[1] Biomedical Engineering Graduate Program, Graduate School of Natural and Applied Sciences
[2] Department of Electrical and Electronics Engineering, Middle East Technical University, 06800, Ankara, Turkey

Abstract—**Automated segmentation of different tissues on medical images is a crucial concept for medical image analysis. In this study, unsupervised image segmentation problem is generalized as a Mumford-Shah energy minimization problem, and several solution proposals for the problem are investigated. Ambrosio-Tortorelli approximation method is implemented, and the performance of the algorithm on magnetic resonance (MR) images of brain is evaluated. First image used in the experiments is chosen among the ones which contain an edema formation due to a brain tumor, and the second one belongs to a healthy subject on which gray matter/white matter segmentation is aimed. Acquired results are presented in visual, tabular and numerical forms. Results and performance are discussed and quantitatively evaluated.**

Keywords—**Medical image processing, unsupervised image segmentation, brain tumor segmentation, gray matter/white matter segmentation.**

I. INTRODUCTION

Medical image analysis is a critical task in clinical radiology, since results gained by the analysis lead physicians for diagnosis, treatment planning, and verification of administered treatment.

Medical images require sequential application of several image post-processing techniques -such as restoration, regularization, segmentation and registration- in order to be used for quantification and analysis of intended features. These features may correspond to the properties of specific parts of the segmented image -like normal tissues, edemas, tumors, or lesions- as well as they may correspond to any statistical property over the entire image domain or over parts of it.

There are many image segmentation algorithms in literature which can be directly used (or adopted into a form that can be used) in medical image domains. However, effective use of many of these methods requires remarkable amount of manual interaction. This situation creates several negations such as difficulty in use and diversity on acquired results. Use of classification based segmentation algorithms requires prior knowledge about class labels, in our case distinct regions of the image. On the other hand, purely clustering based methods suffer from high dependency to the image properties such as noise and/or texture characteristics. Therefore, use of segmentation algorithms falling directly into one of these classes generally involves input dependency, which leads to high standard deviation in results gathered with different parameter sets or images.

In scope of this study, Mumford-Shah based definition of segmentation problem [1] is introduced, a previously established solution to the emphasized problem, approximation of Ambrosio and Tortorelli [2] is implemented and applied on selected brain MR images for unsupervised segmentation of abnormal and different tissues, and the experimental results are analyzed.

Proposed method has previously been used for PET reconstruction, blood cell segmentation [4], denoising and segmentation of brain MR images for white matter-gray matter separation [5], and vascular segmentation and skeletonization [6].

II. BACKGROUND

A. Mumford-Shah Functional

Mumford and Shah described the segmentation problem as minimization of the energy functional:

$$E = \beta \iint_R (u-z)^2 + \alpha \iint_{R-B} |\nabla u|^2 + \iint_R l(B) \qquad (1)$$

Equation (1) defines an energy functional which is formed by summation of three terms. Here, z and u are the functions which are representing the original image and the piecewise smooth (segmented) image, respectively. R denotes the complete image domain. Hence, $\iint_R (u-z)^2$ multiplied by a weighting factor of β (a positive real constant), constitutes a measure for dissimilarity of the segmented image to the original one. Therefore, the first term on the right hand side of (1) is usually called as "*data fidelity term*".

B stands for set of points which compose the boundaries of the segmented image. As a consequence, $R - B$ domain, over which $|\nabla u|^2$ is integrated, is the set of non-boundary points in the segmented image. $|\nabla u|^2$ is an inverse measure for smoothness inside the partitions separated with image boundaries. Ideally (for a purely cartoonized image), second term on the right hand side of (1) is equal to zero. Multiplied by a positive real weighting factor α, the term is ordinarily named as "*regularization term*".

L.M. Roa Romero (ed.), *XIII Mediterranean Conference on Medical and Biological Engineering and Computing 2013*,
IFMBE Proceedings 41,
DOI: 10.1007/978-3-319-00846-2_66, © Springer International Publishing Switzerland 2014

Third building block of Mumford-Shah energy functional gives the total length of the boundaries over the segmented image. Boundaries are the regions which create highest gradient over the piecewise smooth image domain. Observing from linear diffusion perspective, value of the third term approaches to zero with time (in more realistic terms, with iterations), and finally vanishes. This banishes the image from its original state. Therefore, minimizing the third term contradicts with minimization of the data fidelity term. Hence, minimization of the Mumford-Shah energy functional as a whole, transfers the image into an equilibrium state between restoration and regularization processes.

B. Proposed Solutions

Several procedures are proposed for minimization of Mumford-Shah energy functional in references [7,8] and [9]. Referred studies involve utilization of simulated annealing, graph cut algorithms, level set (spline) methods, convex relaxation approaches, and finite-difference discretization for image segmentation based on minimization of Mumford-Shah functional.

Each of these algorithms work well in practice although they have various important drawbacks, such as converging to local minimums, not allowing open boundary formation, and excessiveness of the number of iterations to reach a convergence criterion.

C. Ambrosio-Tortorelli Approximation

In [2], Ambrosio and Tortorelli proposed an approximation for the Mumford-Shah energy functional (Equation (1)), which allows formation of open boundaries, in this sense, is more appropriate with the nature of the original energy, respectively. They proposed to replace the boundary-set term by means of defining a 2D function v and designed the phase field energy functional given below:

$$L_{v,\rho} = \iint_R \{\rho|\nabla v|^2 + (1-v)^2/4\rho\} d\boldsymbol{x}. \qquad (2)$$

In (2), ρ denotes a small positive real number and $\boldsymbol{x}$ is the coordinate vector over 2D image domain.

Although function v cannot be expressed mathematically in an explicit manner, it can be defined and perceived as given by (3):

$$\lim_{\rho\to 0} \frac{1}{2} \iint \{\rho|\nabla v|^2 + v^2/\rho\} = length(B). \qquad (3)$$

If the edge term $\iint_R length(B)$ in original Mumford-Shah energy functional is replaced with the phase field energy term $L_{v,\rho}$ given in (2), and the resulting equation is reorganized such that all terms of integration fall onto the same domain, we end up with the Ambrosio-Tortorelli approximation of Mumford-Shah energy functional, E_{AT} given in (4):

$$E_{AT} = \iint \begin{bmatrix} \beta(u-z)^2 + \alpha|\nabla u|^2(1-v)^2 + \\ (1/2)\{\rho|\nabla v|^2 + (v^2/\rho)\} \end{bmatrix} d\boldsymbol{x}. \qquad (4)$$

Equation (4) has discrete numerical solutions for u and v both of which can be factorized in partial differential equation (PDE) form. The reader is referred to [13, 14] for PDE forms and to [10] for detailed derivations of implicit expressions for u and v.

III. EXPERIMENTAL RESULTS & DISCUSSION

Image segmentation experiments are done with two brain MRI images. The first image is a 1.5 Tesla T2-weighted FLAIR MRI image[1] (size=288x288 pixels, TR=9000 ms, TE=100 ms, pixel spacing=0.79861/0.79861 mm, flip angle=90°, and acquisition parameters=256/191) which belongs to a subject with edema related to brain tumor. A former study with brain MR images which involve MS (multiple sclerosis) lesion formation is previously performed and the results are published in [14]. The second image -which is chosen randomly from the MRI image database of LONI[2]- (T1-weighted MRI) belongs to a healthy male subject, and automated separation of gray matter and white matter of the brain is aimed.

A. Edema Related to Brain Tumor

Edema formation related to brain tumor is often associated with neurologic dysfunction and lowered quality of life. Therefore, it is crucial for the physician to be able to follow-up its progression. Cross-sectional area of the region with edema on a 2D image is one of the most discriminative features for the evaluation of progress. However, manual techniques necessitate more labor, as well as they're more prone to errors originating from subjective assessment.

Although the image in Figure 1 (a) contains an easily observable edema, it is not that straightforward to determine the exact position of boundary pixels, because of the smoothness of boundaries and complex shape of the region.

Aim of the experiments is to test the convergence of the algorithm in image domain with meaningful results. Algorithm is applied on selected region of interest (ROI) shown in Fig 1 (b) with the input parameters presented on first three rows of Table 1. Resulting image is given in Figure 1 (c), which is a piecewise-smooth version of the original image. Boundaries of brain and tumor can easily be examined from the boundary-set given in Figure 1 (e) and they are marked by green curve on Figure 1 (d). Figure 1 (f) shows the region inside the boundary surrounding the brain, but outside the tumor region.

[1] PHILIPS Medical Systems.PHILIPS DICOM Image Server.[Online].
[2] Laboratory of Neuro Imaging at UCLA.(2009) Segmentation Validation Engine.[Online].

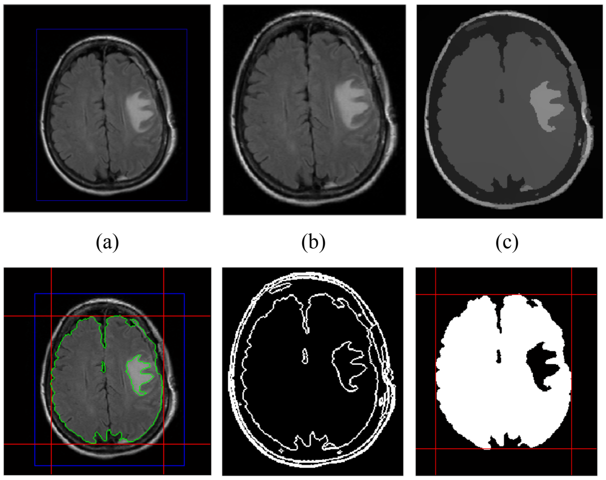

(a) (b) (c)

(d) (e) (f)

Fig. 1 (a) Original brain MR image with edema (b) Selected ROI (c) Segmented image (d) ROI, rectangular area surrounding brain tissue and region boundaries are labeled (e) Visual representation of v function (f) Binary representation of the selected area.

Table 1 Information regarding segmentation of image with edema

INPUTS	Regularization Factor	100	
	Data Fidelity Factor	10	
	Edge Complexity Term	0.05	
OUTPUTS	Iteration Count	20000	
	SSD (Rate of change)	$1.237e^{-003}$	$9.695e^{-006}$
	Mean Value (ROI)	0.195	0.195
	Standard Deviation (ROI)	0.164	0.156
	Entropy (ROI)	6.090	4.189
	Total MS Energy	$2.263e^{005}$	$6.231e^{004}$

Table 2 Information regarding distance and area computation

METADATA	Pixel X-Size	0.79861 mm
	Pixel Y-Size	0.79861 mm
	Slice Thickness	5 mm
COMPUTATIONS	Max Distance (X-Axis)	40 px
		31.9444 mm
	Max Distance (Y-Axis)	57 px
		45.5208 mm
	Cross-Sectional Area	1154 px
		735.9978 mm^2
	Volume On Slice	3679.9888 mm^3

Lower part of Table 1 shows statistical outputs of the procedure. Since Neumann Boundary Condition [11] is considered in the algorithm design stage, whole process appears to be mean preserving. Stopping condition is defined as Sum of Squared Differences (SSD) being smaller than e^{-5}. Decrease in standard deviation and entropy values are reasonable since the aim of the process is lowering the complexity by eliminating noise and texture components over the image. Total Mumford-Shah energy is also reduced significantly.

Two images given in Figure 2 are produced by using same set of input parameters, but just altering the selected region at the last step. This time, region representing the edema is selected and extracted. Computations of horizontal and vertical maximum distances along the abnormal region, cross-sectional area, and volume on slice are handled automatically using DICOM metadata parameters. Results are given on Table 2 in both pixel units and real metrics.

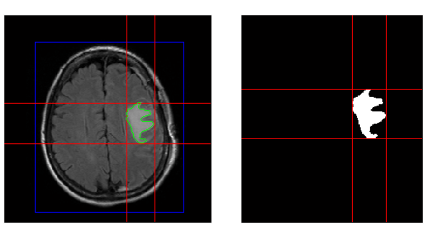

(a) (b)

Fig. 2 (a) ROI and boundaries are labeled for edema region (b) Binary representation of the edema region.

B. Gray Matter/White Matter Segmentation

For the purpose of performance evaluation, an original brain MRI image (Figure 3 (a)) and its ground truth segmented version (Figure 3 (c)) are acquired from Segmentation Validation Engine of Laboratory of Neuroimaging at UCLA. The challenge here is to extract the white matter region from the image in selected ROI.

Algorithm is applied for the ROI shown by blue rectangle on Figure 3 (b). Resulting boundary set is labeled on the same figure. Figure 3 (d) shows the white matter of the right hemisphere of the brain in binary form.

In [12], several metrics for validation of segmentation is introduced. 6 of them, namely, Jaccard Similarity, Dice Coefficient, Sensitivity, Specificity, False Negative Rate (FNR), and False Positive Rate (FPR) are selected among those metrics. Values for aforementioned metrics are calculated using the number of true positives, false positives, true negatives, and false negatives by pixel by pixel comparison of ground truth image and the resulting image

Acquired results of performance evaluation step are presented on Table 3. As observed, total ratio of false decisions to all decisions is under 0.08. It is also seen that value of dice coefficient is above 0.9, and values of sensitivity and specificity are higher than acceptable level.

IV. CONCLUSIONS

One of the most crucial steps in the analysis of brain MRI images for tissue abnormalities is the image

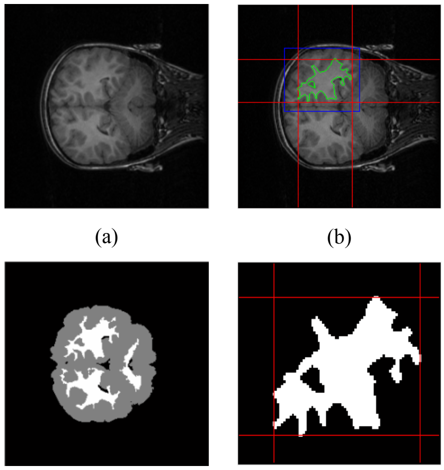

(a) (b) (c) (d)

Fig. 3 (a) Original brain MR image of healthy subject (b) Boundary set and the ROI is marked (c) Ground truth segmented image (d) Binary result of white matter segmentation.

Table 3 Performance evaluation measures for gray matter/white matter separation

Jaccard	0.851810	Specificity	0.969430
Dice	0.919970	FNR	0.045817
Sensitivity	0.954182	FPR	0.030574

segmentation step. Efficient use of an unsupervised algorithm increases accuracy and robustness. It also enables non-specialized physicians to acquire standardized results independent from input variance. A variant of Mumford-Shah based segmentation is applied on sample brain MR images in order to question and observe these facts.

It is observed that Ambrosio-Tortorelli approximation to Mumford-Shah based segmentation is appropriate for segmentation of soft tissues, since it results with an accuracy of higher than 92% and sensitivity and specificity of higher than 95%. It is also important for the algorithm to allow open boundary formation, preserve the average gray-level, and provide robustness by constituting a balance between regularization and restoration on the basis of degree of complexity in the image domain.

Search for relations between data fidelity and regularization constants and optimality criteria in selection of those are considered as our following studies in the field.

ACKNOWLEDGMENT

This study is based on Alper Çevik's M.Sc. thesis and B. Murat Eyüboğlu is the thesis supervisor. This research project has been supported by the Graduate School of Natural and Applied Sciences, METU Scientific Research Fund "BAP 07-02-2012-101".

REFERENCES

1. Mumford, D. and Shah, J., "Optimal approximations by piecewise smooth functions and associated variational problems," *Communications on Pure and Applied Mathematics*, vol. 42, no. 5, pp. 577--685, 1989.
2. Tortorelli, V.M. andAmbrosio, L., "Approximation of functional depending on jumps by elliptic functional via t-convergence," *Communications on Pure and Applied Mathematics*, vol. 999-1036, p. 43, 1990.
3. Zhou, J.,Shu, H., Xia, T.,Luo, L., "PET Image Reconstruction Using Mumford-Shah Regularization Coupled with L^1Data Fitting," *Engineering in Medicine and Biology Society, 2005. IEEE-EMBS 2005. 27th Annual International Conference of the* , vol., no., pp.1905-1908, 17-18 Jan. 2006
4. Lin, P., Yan, X.,Zheng, C., Yang, Y., "Medical image segmentation based on Mumford-Shah model," *Communications, Circuits and Systems, 2004. ICCCAS 2004. 2004 International Conference on* , vol.2, no., pp. 942- 945 Vol.2, 27-29 June 2004
5. Du, X., Bui, T.D., "Image segmentation based on the Mumford-Shah model and its variations," *Biomedical Imaging: From Nano to Macro, 2008. ISBI 2008. 5th IEEE International Symposium on* , vol., no., pp.109-112, 14-17 May 2008
6. Lam, B.S.Y., Yan, H., "Blood Vessel Extraction Based on Mumford Shah Model and Skeletonization," *Machine Learning and Cybernetics, 2006 International Conference on* , vol., no., pp.4227-4232, 13-16 Aug. 2006
7. Cremers, D., Tischhauser, F., Weickert, J. and Schnorr, C., "Diffusion snakes: introducing statistical shape knowledge into the Mumford-Shah functional," *J. OF COMPUTER VISION*, vol. 50, 2002.
8. Vese, L.A. and Chan, T.F., "A Multiphase Level Set Framework for Image Segmentation Using the Mumford and Shah Model," *International Journal of Computer Vision*, vol. 50, pp. 271-293, 2002.
9. Chambolle, A., "Finite-differences discretizations of the Mumford-Shah functional," *M2AN*, vol. 33, no. 2, pp. 261-288, 1999.
10. Erdem, E., Sancar-Yilmaz, A. and Tari, S., "Mumford-Shah regularizer with spatial coherence," in *Proceedings of the 1st international conference on Scale space and variational methods in computer vision*, Berlin, Heidelberg, pp. 545-555, 2007.
11. Cheng, A. and Cheng D. T.,"Heritage and early history of the boundary element method", *Engineering Analysis with Boundary Elements*, 29, 268–302. 2005.
12. Shattuck, D. W., Prasad G., Mirza M., Narr K. L., and Toga A. W., "Online resource for validation of brain segmentation methods," *NeuroImage*, vol. 45, no. 2, pp. 431-439, 2009.
13. Cevik, A.,"A Medical Image Processing and Analysis Framework,"Master's thesis, Biomedical Engineering Graduate Program,Middle East Technical University, Ankara, Turkey, 2011.
14. Cevik, A., Eyuboglu B. M., "Doku Anomalisi İçeren Beyin MR İmgeleri Üzerinde Mumford-Shah Tabanlı Bölütleme," EMO Bilimsel Dergi, vol. 1, no. 2, pp. 103-107, 2011.

Author: Alper Çevik
Institute: Middle East Technical University
Street/City/Country: METU/Ankara/Turkey
Email: alper.cevik@metu.edu.tr